

Elsevier Editorial System(tm) for Nuclear Inst. and Methods in Physics Research, A
Manuscript Draft

Manuscript Number:

Title: Bi-spectral extraction through elliptic neutron guides

Article Type: Research Paper

Section/Category: Accelerators, Beam Handling and Targets

Keywords: bi-spectral neutron beam extraction; neutron instrumentation; supermirror; European Spallation Source; elliptic neutron guide; ray-tracing simulations; ESS; McStas; VITESS; iFit

Corresponding Author: Mr. Henrik Jacobsen, B.sc.

Corresponding Author's Institution: Niels Bohr Institute

First Author: Henrik Jacobsen, B.sc.

Order of Authors: Henrik Jacobsen, B.sc.; Klaus Lieutenant; Carolin Zendler; Kim Lefmann

Abstract: In this article we present the results of investigating a suggested guide extraction system utilizing both a thermal and a cold moderator at the same time, the so-called bi-spectral extraction. Here, the thermal moderator has line of sight to the sample position, and the neutrons from the cold source are reflected by a supermirror towards the sample.

The work is motivated by the construction of the European Spallation Source (ESS) but the results are general and can be used at any neutron source. Due to the long pulse structure, most instruments at ESS will be long, often exceeding 50 m from moderator to detector. We therefore investigate the performance of bi-spectral extraction for instrument lengths of 30 m, 56 m, 81 m and 156 m. In all these cases, our results show that we can utilize both moderators (and thus high intensity in a wide wavelength band) in the same instrument at a cost of flux of 5-25 % for neutrons with wavelength larger than 1 Å. In general, the divergence distribution is smooth at the sample position.

Bi-spectral extraction through elliptic neutron guides

Henrik Jacobsen^{a,b,*}, Klaus Lieutenant^c, Carolin Zendler^c, Kim Lefmann^{a,b}

^a*Nanoscience center and eScience center, Niels Bohr Institute, University of Copenhagen*

^b*ESS design update program, Denmark*

^c*Helmholtz-Zentrum Berlin, Hahn-Meitner-Platz 1, D-14109 Berlin, Germany*

Abstract

In this article we present the results of investigating a suggested guide extraction system utilizing both a thermal and a cold moderator at the same time, the so-called bi-spectral extraction. Here, the thermal moderator has line of sight to the sample position, and the neutrons from the cold source are reflected by a supermirror towards the sample.

The work is motivated by the construction of the European Spallation Source (ESS) but the results are general and can be used at any neutron source. Due to the long pulse structure, most instruments at ESS will be long, often exceeding 50 m from moderator to detector. We therefore investigate the performance of bi-spectral extraction for instrument lengths of 30 m, 56 m, 81 m and 156 m. In all these cases, our results show that we can utilize both moderators (and thus high intensity in a wide wavelength band) in the same instrument at a cost of flux of 5-25 % for neutrons with wavelength larger than 1 Å. In general, the divergence distribution is smooth at the sample position for all wavelengths.

Keywords:

*Corresponding author

Email address: hjacobse@fys.ku.dk (Henrik Jacobsen)

bi-spectral neutron beam extraction, neutron instrumentation, supermirror, European Spallation Source, elliptic neutron guide, ray-tracing simulations, ESS, McStas, VITESS, iFit

1. Introduction

The long-pulsed European Spallation neutron source, the ESS, is presently in planning [1]. Due to the long pulse, most instruments will be long, exceeding 50 m from moderator to detector. For the design of instruments for the ESS, much assumed knowledge is presently being re-investigated. One important part is the neutron guide system, where elliptical guides are being considered for many instruments. Much effort is currently put into understanding how elliptic guides transport neutrons [2–4]. A particular challenge is the design of the first few meters; the so called guide extraction system.

Bi-spectral extraction, as first proposed by Mezei and Russina [5–7] is being considered for several instruments. This system is already implemented at the EXED [8] beam line at HZB, and is shown to work well with straight guides. However, there has been much discussion whether bi-spectral extraction will work equally well with elliptic guides, which is the subject of this work.

A sketch of uni- and bi-spectral extraction is given in Fig. 1. For detailed information about uni-spectral extraction, see e.g. the work of Klenø et. al [2].

In the bi-spectral extraction system, a cold and a thermal moderator are located next to each other. A supermirror reflects the neutrons from the cold source into the guide while neutrons from the thermal source are able

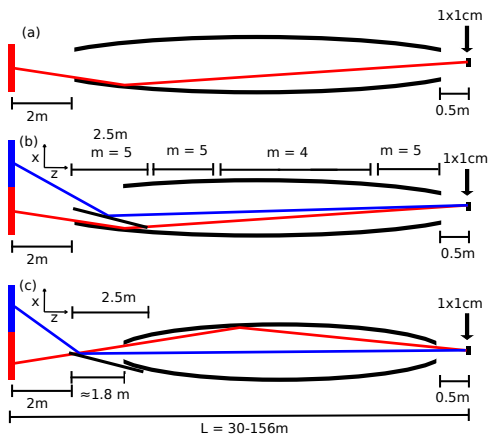


Figure 1: (Color online) Sketch of (a) uni-spectral and (b-c) bi-spectral extraction with elliptic guides. Top view. The minor axes of the ellipses is greatly exaggerated for clarity. (b) illustrates the expected optimal settings with the mirror inside the guide, while (c) illustrates a typical optimum found in this work.

22 to pass through the mirror into the guide. As discussed below, supermirrors
 23 reflect neutrons below a critical scattering vector given by mq_c , where in
 24 our case $m = 4$ and $q_c = 0.0217 \text{ \AA}^{-1}$ is the critical scattering vector of
 25 nickel. Therefore, most of the thermal neutrons pass through the mirror
 26 due to their large k -vectors and the low absorption in the mirror. Thus the
 27 mirror can be seen as a switch between the two moderators, that activates the
 28 cold moderator and deactivates the thermal moderator when the wavelength
 29 is increased above a certain cross-over wavelength. Ideally, the cross-over
 30 should be near $\lambda_c \approx 2.5 \text{ \AA}$ where the brilliance curves of the two moderators
 31 meet. This makes it possible to utilize a wide range of incoming neutron
 32 wavelengths.

33 Of course, the cross-over wavelength depends on incident angle of the
 34 neutron velocity with respect to the mirror, and is therefore different for

35 different parts of the two moderators. So the switching from the thermal
36 to the cold moderator happens gradually near $\lambda = 2.5 \text{ \AA}$, and close to this
37 wavelength, neutrons from both moderators will reach the sample. Even so,
38 it is here worth noting that, for any given wavelength and divergence, the
39 theoretically highest intensity at the sample is the maximum of the intensity
40 of the cold and the thermal source, and not the sum of the two, as one
41 might expect. This follows directly from Liouville's theorem [9]. See also the
42 discussion of (Eq. 4).

43 **2. Introduction to the simulations**

44 To investigate the extraction system in detail, we have simulated the set-
45 up using the Monte Carlo neutron ray-tracing packages McStas [10, 11] and
46 VITESS [12, 13].

47 The optimizations and data plotting for McStas data were performed
48 using iFit [14, 15]. The computations were carried out on the 500 core cluster
49 of the ESS Data Management and Software Center [16]. As an example,
50 the optimization and subsequent simulation of the results shown in Fig. 3
51 took approximately 1 day on a 12 core node of the cluster. For VITESS
52 simulations, the HZB cluster was used [17].

53 In the following we will briefly outline the instrument, and discuss which
54 parameters are fixed and which are optimized in these simulations.

55 The moderator characteristics used are the standard ESS sources provided
56 in McStas 1.12c, with a slight modification of the cold source in order to direct
57 the beam to the guide entrance to save simulation time. The temperature
58 of the thermal source is 325 K, that of the cold source is 50 K. The size of

59 both sources is $12 \times 12 \text{ cm}^2$; the thermal source is placed at $(0,0,0)$, The
60 cold source at $(0.12,0,0)$. The mirror is 2.5 m long, starting 2.0 m after
61 the thermal source. It is inclined approximately 1.25° relative to the beam
62 direction. This angle is optimized in the simulations.

63 The sample is $1 \times 1 \text{ cm}^2$ and is placed 0.5 m from the end of the elliptic
64 guide.

65 The implementation of the elliptic guide in these simulations is the one
66 designed by Kaspar Klenø [2], consisting of 50 `Guide_gravity` components.

The coating of the guide and the mirror plays a crucial role in these simulations. The standard description of the reflectivity in version 1.12c McStas assumes constant reflectivity for $q < q_c$ (we here use $R_0 = 0.99$), a linear decrease of reflectivity with a certain slope, α (typically $\alpha = 3.5$) followed by a sharp cutoff with width W around mq_c , where $1 < m < 7$ is the m -value of the mirror:

$$R(q) = R_0 (1 - \alpha(q - q_c)) \tanh\left(\frac{q - mq_c}{W}\right). \quad (1)$$

It turns out that the linear decrease in this model is too simple and does not accurately describe real mirrors. To improve the description, reflectivity curves for 7 state-of-the-art mirrors with different m -values, provided by Swiss Neutronics [18], were fitted to the following generalization of the model

$$R(q) = R_0 \left(1 - \alpha(q - q_c) + \beta(q - q_c)^2\right) \tanh\left(\frac{q - mq_c}{W}\right). \quad (2)$$

67 The values of α , β and W were extracted and found to a good approximation
68 to depend linearly on m . We thus arrived at a model of the reflectivity

69 that accurately describes real mirrors and requires only m as input. The
70 reflectivity curves as function of q are shown along with the data for $m = 2$,
71 $m = 3$, $m = 4$, $m = 5$, $m = 6$ and $m = 7$ in Fig. 2. It is here worth noting
72 that, contrary to the version 1.12c McStas model, larger values of m do not
73 always lead to more neutrons being reflected by the mirror: although the
74 reflectivity is non-zero for larger values of q , it is significantly lower for low
75 values of q .

76 This model will be the default in McStas 2.1 [11], and can be used in
77 the VITESS guide modules by generating reflectivity files with the according
78 tool in VITESS 3 or higher [13]. In the `sm_ensemble` module, the reflectivity
79 and attenuation have been changed to match the McStas models, which will
80 be available in VITESS from version 3.1 onwards.

81 Based on these considerations, an optimization of the optimal coating
82 for a 156 m instrument showed that optimal transfer of neutrons is achieved
83 when the coating of the guide is $m = 5$ for the first and last 15 parts of
84 the guide near the ends and $m = 4$ in the middle. For a 156 m instrument,
85 the $m = 5$ coating covers approximately the first 15 m and last 12 m. For
86 a 56 m instrument, the $m = 5$ coating covers approximately the first 7 m
87 and last 5 m. Of course it is very expensive to construct a 156 m guide with
88 $m \geq 4$ throughout. For most of the guide, lower m -values can be used with
89 essentially no loss of neutrons, as shown by Refs. [19, 20]. Optimizing the
90 cost of the guide is, however, not the purpose of this paper, and we therefore
91 use these high m -values.

92 The optimal values for the horizontal and vertical focal points and small
93 axis widths all depend on the exact set-up and figure of merit for the sim-

94 ulations, and therefore need to be optimized. In some of the optimizations,
95 the optimal settings for the neutrons from the cold moderator will make the
96 guide opening width/height very small, drastically reducing the intensity of
97 the neutrons from the thermal source. To compensate for this, the start po-
98 sition of the guide has also been optimized. This effect is illustrated in Fig. 1
99 c.

100 Perhaps the most important component in these simulations is the mir-
101 ror. The McStas `Mirror` component does not take absorption into account,
102 and therefore a new mirror component has been written (`curved_mirror`).
103 Initially, the coating was chosen to be $m = 5$, but with the description of the
104 coating according to (Eq. 2), $m = 4$ performs better than $m = 5$, and has
105 therefore been used. The mirror is modeled as a $t_c = 10 \mu\text{m}$ thin supermir-
106 ror layer with 50% Titanium and 50% Nickel on top of a $t_s = 0.5 \text{ mm}$ thick
107 sapphire substrate, in which refraction and attenuation due to absorption
108 and inelastic incoherent scattering are taken into account [21]. For details
109 see Fig. 2. As an example, a 1 \AA neutron reaching the mirror with an angle
110 $\theta_1 = 1.25^\circ$ will be attenuated by approximately 7 %.

111 It should here be noted that it is possible that some of the mirror is
112 located inside the guide, where it fills out the guide completely in the vertical
113 direction (out of the plane in Fig. 1 (b)). This is not supported by the
114 standard guide components in McStas. To implement this, an elliptic guide
115 wall component (`elliptic_mirror`) has been written and is used to model
116 each wall of the guide for the first few meters. As illustrated in Fig. 1,
117 the guide wall facing the cold source is shorter than the others, to allow the
118 neutrons from the cold source to reach the mirror. This means that the order

119 of the components is not uniquely defined, as is normally the case in McStas.
120 Correct propagation of the neutrons is thus realized by a generalization of
121 the method described in [22].

122 We have investigated the effect of curving the mirror, and have come to
123 the conclusion that almost no gains are possible. We have also tried varying
124 the m -value along the mirror, also with no gains. To limit the investigated
125 parameter space, we therefore work with a flat mirror with the same m -value
126 throughout.

127 For the VITESS simulation, the same moderator and material charac-
128 teristics were used. The only difference is that the thickness of the su-
129 permirror layer on the mirror is not explicitly considered. The module
130 `supermirror_ensemble` has been used to simulate the mirror and the guide
131 system around the mirror.

We have analyzed this set-up using several different figures of merit. First
of all, the instrument will be compared to the standard uni-spectral extrac-
tion. In general, the usable wavelength bands, $\delta\lambda$, depend on the length of
the instrument and the time structure of the source according to

$$\delta\lambda = \frac{T}{\alpha L}, \quad (3)$$

132 where T is the moderator period ($T = 71.4$ ms for ESS), L is the length of
133 the instrument and $\alpha = m_n/h = 252.7\mu\text{s}/\text{m}/\text{\AA}$. We here investigate 4 of
134 the standard lengths considered for ESS [23]: 30 m, 56 m, 81 m and 156
135 m, corresponding to $\delta\lambda = 9.4, 5.0, 3.5$ and 1.8 \AA, respectively. The main
136 question is how well the set-up performs for cold neutrons. We have chosen
137 to restrict the wavelength bands somewhat for the short instruments, and
138 have thus optimized the following 'cold' wavelength bands: 30 m: 3.0 – 7.5

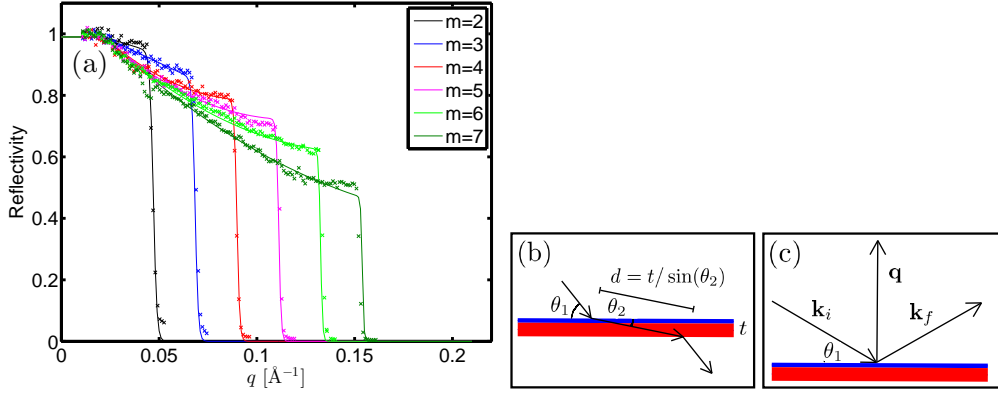


Figure 2: (Color online) Model of the mirror. (a) the reflectivity for different m -values as function of scattering vector, q . The data points are measurements by Swiss Neutronics and the solid lines are the model (Eq. 2) (b) and (c): The mirror consists of a thin coating (blue) on top of a thicker substrate (red). (b) illustrates how absorption and refraction are taken into account, while (c) illustrates reflections.

139 \AA , 56 m: 3.0 – 7.5 \AA , 81 m: 3.25 – 6.75 \AA , 156 m: 4.1 – 5.9 \AA .

140 The virtue of bi-spectral extraction is the possibility to utilize a wide
 141 wavelength band. We have therefore also optimized the instrument in the
 142 'full' wavelength band 0.75 – 7.25 \AA . Finally, the overlap region near 2.5 \AA ,
 143 where the brilliance is the same for the two moderators, is of special interest.
 144 We have therefore also optimized the set-up within 1-4 \AA , here named the
 145 'bi-spectral' wavelength band.

146 Each of these optimizations have been carried out for three different limits
 147 for the divergence at the sample position, as previously studied by e.g. Ref.
 148 [2] : $\pm 0.5^\circ$, $\pm 1.0^\circ$ and $\pm 2.0^\circ$. This gives a total of 36 optimizations of bi-
 149 spectral extraction and 24 optimizations of uni-spectral extraction.

150 Optimizing absolute intensities does not produce satisfactory results, as
 151 the intensity of 1.5 \AA is much higher than e.g. 5 \AA neutrons. We have

152 therefore optimized the brilliance transfer, $B(\lambda, D)$ instead. Brilliance is
 153 defined as number of neutrons per second, per square centimeter, within a
 154 wavelength band λ , within a divergence limit (D). Brilliance transfer, then,
 155 is the ratio of brilliance at the sample and the source. The virtue of this is
 156 that all wavelengths are weighted equally.

157 For any given λ and D , the bi-spectral source brilliance $B_{\text{bi}}(\lambda, D)$ is the
 158 maximal brilliance of the two moderators. Naming the brilliance of the cold
 159 source $B_{\text{c}}(\lambda, D)$ and that of the thermal source $B_{\text{t}}(\lambda, D)$, we thus have

$$B_{\text{bi}}(\lambda, D) = \begin{cases} B_{\text{t}}(\lambda, D) & \text{for } \lambda < \lambda_{\text{c}} \\ B_{\text{c}}(\lambda, D) & \text{for } \lambda > \lambda_{\text{c}}. \end{cases} \quad (4)$$

160 We note again that Liouville's theorem [9] states that the brilliance trans-
 161 fer can never exceed 100%. This makes $B(\lambda, D)$ a direct measure of the
 162 quality of the guide system.

163 The majority of the results will be given in terms of brilliance transfer
 164 instead of absolute intensities, and are therefore of general validity, also for
 165 other sources than ESS.

166 **3. Results**

167 *3.1. Wavelength distribution*

168 Fig. 3 shows an example of the simulated intensity as a function of wave-
 169 length on a $1 \times 1 \text{ cm}^2$ sample for neutrons with divergence less than 0.5° .
 170 The best results that can be obtained with uni-spectral extraction are shown
 171 for comparison.

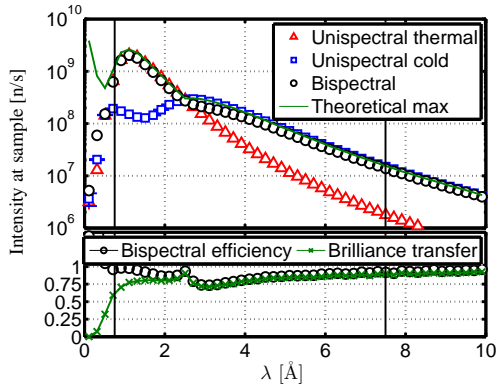


Figure 3: (Color online) The wavelength distribution at the sample, comparing the performance of bi-spectral extraction to a normal uni-spectral extraction system for a 156 m instrument for neutrons with divergence within $\pm 0.5^\circ$. The vertical lines show the limits of the wavelength band used in the optimizations. The lower panel shows brilliance transfer and efficiency compared to uni-spectral extraction.

172 In the lower panel, the brilliance transfer and efficiency are plotted. Ef-
 173 ficiency at a given wavelength is defined as the performance compared to an
 174 optimal uni-spectral elliptic guide, and mainly serves to judge the perfor-
 175 mance below 1 Å, where the brilliance transfer drops quickly to zero.

176 In this example we see that it is possible to obtain brilliance transfers ex-
 177 ceeding 75% for neutrons with wavelengths larger than 0.75 Å. For neutrons
 178 with wavelengths larger than 6 Å, the brilliance transfer reaches more than
 179 90%. These results depend slightly on which wavelength band has been opti-
 180 mized. Before investigating other wavelength bands and instrument lengths,
 181 we validate the simulations by comparing McStas and VITESS simulations,
 182 as shown in Fig. 4. In this comparison only, the absorption in the coat-
 183 ing of the mirror is neglected in the McStas simulation. It is seen that the
 184 agreement between McStas and VITESS is within 3 % except at $\lambda < 0.6$ Å.

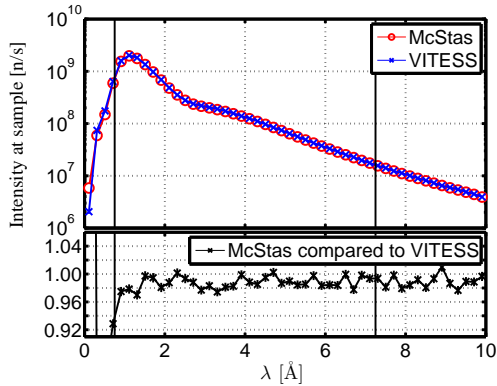


Figure 4: (Color online) The wavelength distribution at the sample for a 156 m instrument for neutrons with divergence within $\pm 0.5^\circ$, comparing McStas and VITESS simulations. The vertical lines show the limits of the wavelength band used in the optimizations. The lower panel shows the ratio of intensity of McStas to VITESS simulations.

185 In Fig. 5 we give an overview of the performance for all the optimizations
 186 mentioned above, showing brilliance transfer as function of wavelength for the
 187 4 different instrument lengths and 3 divergence limits. Each figure contains
 188 five graphs: (—) and (---) show the performance of the thermal and cold uni-
 189 spectral, respectively, when compared to the Liouville limit for the bi-spectral
 190 extraction. The three other graphs show the results when optimizing for the
 191 'cold' (\circ), 'full' (\triangle) and 'bi-spectral' (\square) wavelength bands, respectively.
 192 Much information can be extracted from Fig. 5. A general feature is that for
 193 low divergent neutrons, it is possible to obtain brilliance transfers exceeding
 194 70% for neutrons with wavelength 1 Å or higher. The brilliance transfer of
 195 thermal neutrons can be increased at the cost of cold neutrons and vice versa.
 196 It is not quite possible to reach the performance of two combined uni-spectral
 197 sources throughout the interesting wavelength band, but we can reach 75%
 198 in the overlap region and up to 95% elsewhere.

199 For neutrons with divergence larger than $\pm 0.5^\circ$, brilliance transfers within
200 50-75% can be obtained.

201 In some cases, the optimal settings found by the optimizer is the same
202 for all three figures of merit, and thus one or two of the data sets are not
203 visible.

204 3.2. Divergence distribution

205 Let us now look closer at the neutrons getting through the guide. We will
206 focus on the set-ups that give best overall brilliance transfer of low divergent
207 neutrons ($\pm 0.5^\circ$), i.e. we show the results of the following optimizations: 30
208 m: 'cold', 56 m: 'cold', 81 m: 'bi-spectral', 156 m: 'full'. The divergence
209 of the neutrons should ideally be smooth and symmetric. In Fig. 6 we show
210 the divergence for three different 0.01 Å wide wavelength bands, centered on
211 the following wavelengths: 1.5 Å (\circ), 2.5 Å (\square) and 5.0 Å (\times). In the plot
212 of x (y) divergence, the neutrons with y (x) divergence larger than 0.5°
213 have been removed.

214 There is some structure in the divergence distribution, especially for the
215 30 m instrument, but in general, the divergence is quite smooth within the
216 chosen limits. In some cases, there are a lot of unwanted neutrons, i.e.
217 neutrons with divergence larger than the required limits. These will of course
218 have to be removed, e.g. by replacing the last few meters of the guide with
219 absorbing material, by use of collimators or slits in the guide or by further
220 optimizations. Modification of this detail is, however, not the purpose of this
221 work.

222 There are differences between the divergence distribution in the horizontal
223 (x) and vertical (y) direction. There are three reasons for this. The main

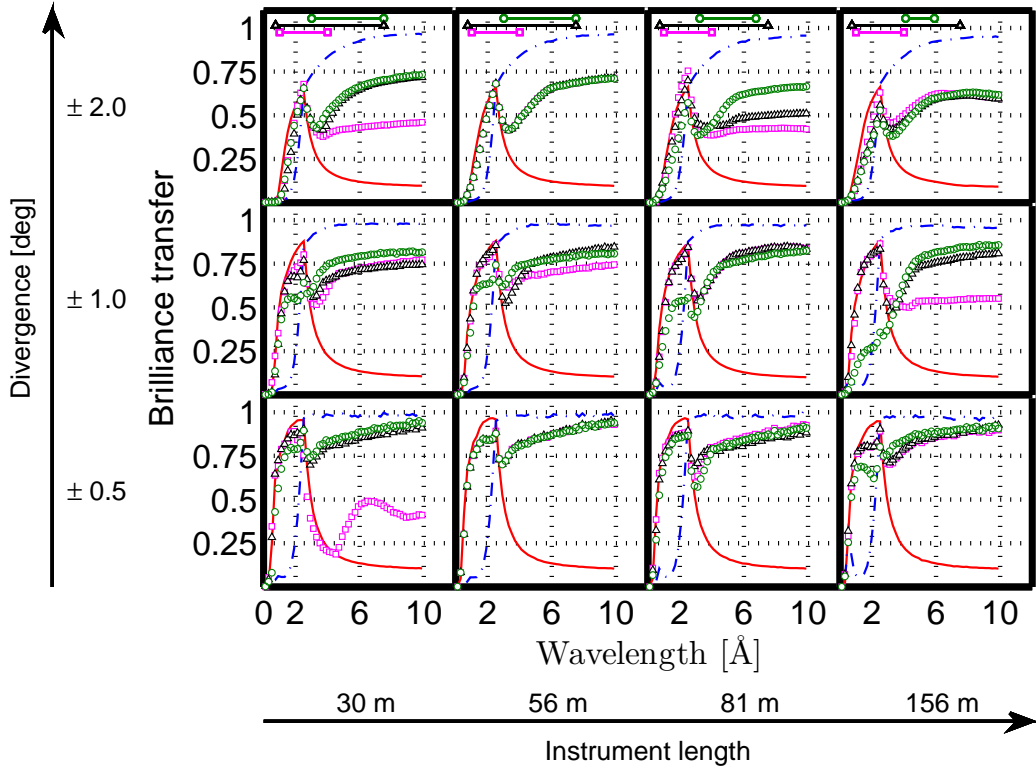


Figure 5: (Color online) Brilliance transfer distribution, optimized for 3 different wavelength bands. (—) and (---) show the performance of the thermal and cold uni-spectral, respectively, when compared to the Liouville limit for the bi-spectral extraction. The three other graphs show the results when optimizing for the 'cold' (\circ), 'full' (\triangle) and 'bi-spectral' (\square) wavelength bands, respectively. The horizontal lines in the top indicate these wavelength bands.

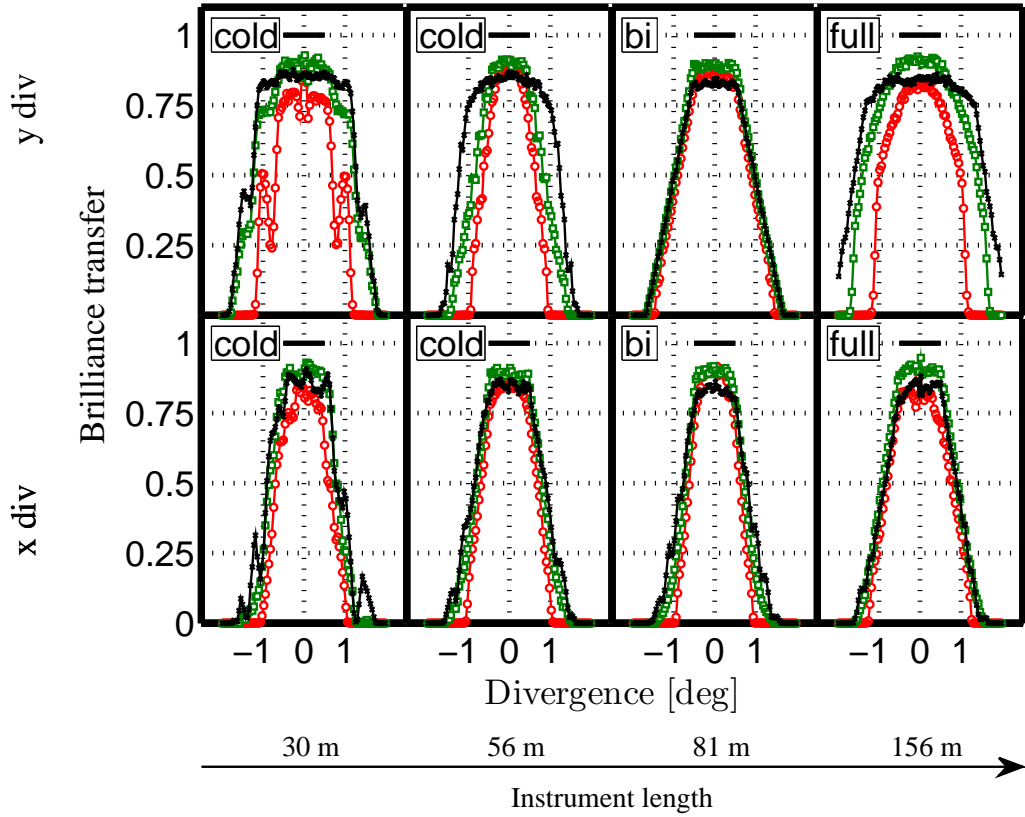


Figure 6: (Color online) Horizontal (x) and vertical (y) divergence for the set-ups with best overall performance, for neutrons with the following wavelengths, 1.5 Å (\circ), 2.5 Å (\square) and 5.0 Å (\times). The horizontal lines show the divergence for which the set-up has been optimized ($\pm 0.5^\circ$), and the text indicates the wavelength band that has been optimized: 30 m: 'cold', 56 m: 'cold', 81 m: 'bi-spectral', 156 m: 'full'. The cross section of the guides is rectangular.

224 reason is that, contrary to e.g. Ref. [2], the cross-section of the guide is
225 not forced to be square. This extra freedom in parameter space has been
226 added because the horizontal and vertical directions are not a priori equal.
227 Secondly, the mirror distorts the divergence in the horizontal direction, and
228 thirdly gravity has a small effect on the vertical direction.

229 In Fig. 7, the same results are shown for an optimization in which the
230 cross section of the guide has been forced to be square. Here, the divergence
231 in the horizontal-direction is not at all pretty, and the intensities are smaller
232 by 5-10%. The loss in intensity can be tolerated, but the uneven divergence
233 distribution could be a problem. We can thus conclude that to limit the
234 negative effects of the mirror, the guide cross section must be rectangular
235 instead of square.

236 3.3. Acceptance diagrams

237 In Fig. 8 we further investigate the 156 m instrument shown in Fig. 3
238 and 6, i.e. optimized for low divergence within the 'full' wavelength band.
239 We focus on 3 wavelengths: 1.5 Å (top), 2.5 Å (center) and 5 Å (bottom).
240 Each figure shows 4 plots: (a) 2d divergence, (b) horizontal acceptance dia-
241 gram (divergence vs position), (c) vertical acceptance diagram, (d) position.
242 The black boxes indicate the sample position and divergence limit. In the
243 dimensions not shown in each figure, only the neutrons that reach the sam-
244 ple with divergence within $\pm 0.5^\circ$ are counted. In the horizontal acceptance
245 diagram, for example, neutrons with vertical divergence larger than $\pm 0.5^\circ$
246 are removed, while in the divergence monitor neutrons outside the 1×1
247 cm² sample position are removed. All the monitors have been normalized to
248 brilliance transfer.

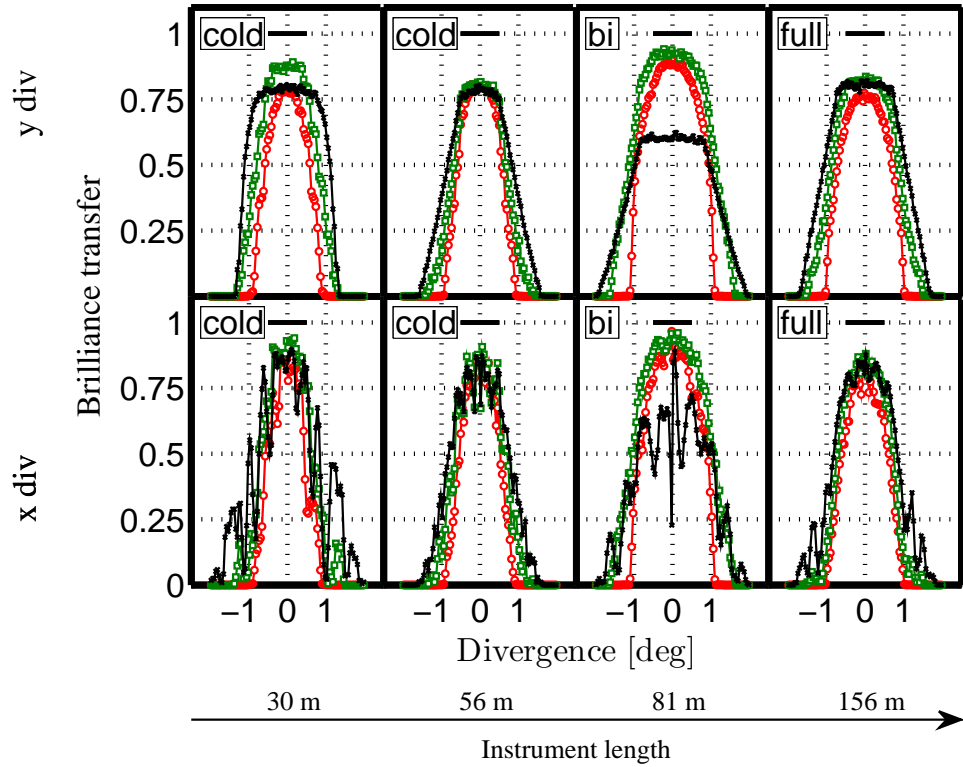


Figure 7: (Color online) Horizontal (x) and vertical (y) divergence for the set-ups with best overall performance when the guide has a square cross section, for neutrons with the following wavelengths, 1.5 \AA (\circ), 2.5 \AA (\square) and 5.0 \AA (\times). The horizontal lines show the divergence for which the set-up has been optimized ($\pm 0.5^\circ$), and the text indicates the wavelength band that has been optimized: 30 m: 'cold', 56 m: 'cold', 81 m: 'bi-spectral', 156 m: 'full'.

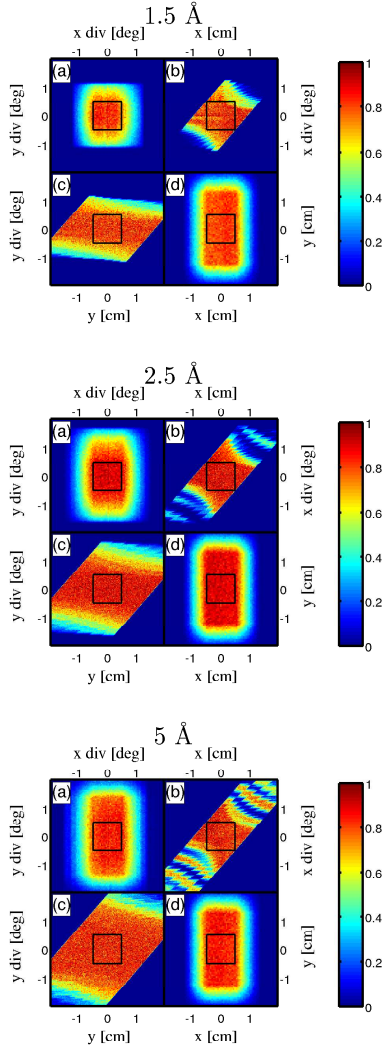


Figure 8: (Color online) Investigation of the properties of neutrons getting through the guide for a 156 m extraction optimized for low divergent neutrons within the 'full' wavelength band. (a) 2d divergence, (b) horizontal acceptance diagram (divergence vs position), (c) vertical acceptance diagram, (d) position. The black boxes indicate the sample position and divergence limit. In the dimensions not shown in each figure, only the neutrons that hit the sample with horizontal (x) and vertical (y) divergence within $\pm 0.5^\circ$ are counted. In the horizontal acceptance diagrams (b), for example, neutrons with vertical divergence larger than $\pm 0.5^\circ$ are removed.

249 It is seen that the beam profile is smooth at the sample position for all
250 wavelengths. It should be noted that many unwanted neutrons reach the
251 sample position.

252 The parameters for this set-up (156 m, low divergence, optimized for 'full'
253 wavelength band) are the following, where all positions are given relative to
254 the center of the thermal moderator: start of guide: 3.86 m, first horizontal
255 focus point: 2.80 m, second horizontal focus point: 156.0 m, largest width
256 of the guide: 16.5 cm, first vertical focus point: -0.05 m, second vertical
257 focus point: 156.6 m, height of guide: 20.1 cm, center position of mirror:
258 -0.9 ± 0.5 cm, inclination of mirror: $1.1 \pm 0.2^\circ$. The uncertainties in the last
259 two numbers are estimates on what error can be tolerated without significant
260 loss of neutrons. This has been found by simulating the specific set-up with
261 varying values of the two parameters. The effect of misaligning the guide has
262 been studied elsewhere [24].

263 Thus, the dimensions of the guide at the start are 2.7×6.4 cm², while
264 at the exit they are 1.9×3.3 cm². It is interesting to note that the optimal
265 position of the mirror is outside the guide as shown in Fig. 1 (c); this was
266 not anticipated from the first results of this work.

267 In Fig. 9 we show the same plots for the 30 m instrument shown in
268 Fig. 3 (i.e. optimized for low divergent neutrons). The neutrons reaching
269 the sample with the wanted divergence in general behave well. A notable
270 exception is the 1.5 Å neutrons, where the intensity is visibly larger on one
271 side of the sample than the other. This is because the path length through the
272 mirror, and therefore the absorption, depends on the incoming angle of the
273 neutrons, which is what determines where the neutrons hit the sample. This

274 effect is not seen in longer guides where the neutrons are reflected several
275 times by the guide before reaching the sample [4]. Another effect for 1.5
276 Å neutrons is some structure in the divergence distribution. However, this
277 appears quite symmetric and therefore should not be a problem for the q -
278 dependent part of the instrument resolution function.

279 The parameters for this set-up are the following, where all positions are
280 given relative to the center of the thermal moderator: start of guide: 3.56
281 m, first horizontal focus point: 2.0 m, second horizontal focus point: 30.5 m,
282 largest width of the guide: 5.7 cm, first vertical focus point: 1.7 m, second
283 vertical focus point: 30.7 m, height of guide: 14.5 cm, center position of
284 mirror: -0.7 ± 0.5 cm, inclination of mirror: $1.1 \pm 0.2^\circ$.

285 Thus, the dimensions of the guide at the start are 2.6×7.2 cm², while at
286 the exit they are 2.0×5.8 cm².

287 Here, it is worth noting that the width of the guide is quite small.

288 4. Discussion and conclusion

289 We have investigated bi-spectral extraction through elliptic guides for
290 4 typical instrument lengths proposed for ESS using McStas and VITESS
291 simulations. Our simulations show that brilliance transfers of more than
292 75% can be achieved for neutrons with wavelength larger than 1 Å. For cold
293 neutrons, brilliance transfers exceeding 90% are obtainable.

294 We have focused on neutrons with relatively low divergence ($\pm 0.5^\circ$), and
295 have found that the divergence profile at the sample position is smooth, as
296 is required by many instrument designers.

297 The figures of merit for these simulations are intensity of neutrons at the

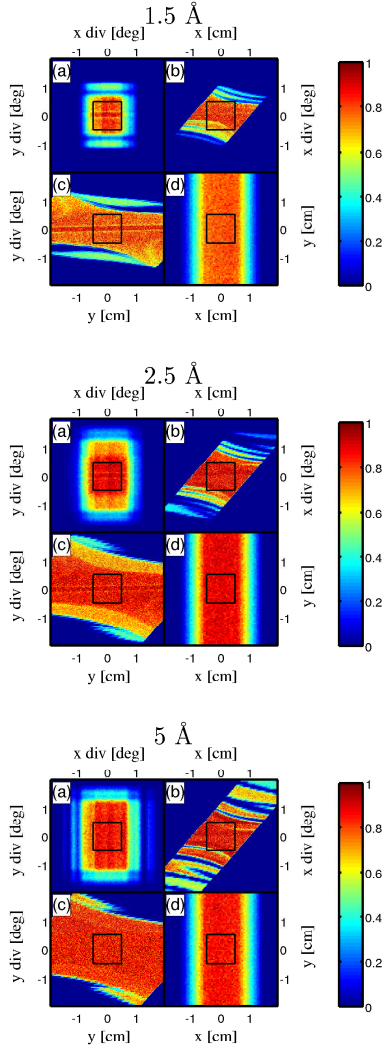


Figure 9: (Color online) Investigation of the properties of neutrons reaching getting through the guide for a 30 m extraction, optimized for low divergent neutrons within the 'cold' wavelength band. (a) 2d divergence, (b) horizontal acceptance diagram (divergence vs position), (c) vertical acceptance diagram, (d) position. The black boxes indicate the sample position and divergence limit. In the dimensions not shown in each figure, only the neutrons that hit the sample with divergence within $\pm 0.5^\circ$ are counted. In the horizontal acceptance diagrams (b), for example, neutrons with vertical divergence larger than $\pm 0.5^\circ$ are removed.

298 sample position within certain divergence limits. Another important require-
299 ment for all instruments is that the background be minimal. Therefore, it
300 is often desired to get out of line of sight. For short instruments this is ob-
301 viously difficult for both uni- and bi-spectral extraction, but not impossible.
302 For longer instrument, using e.g. a double ellipse and a kink in the guide
303 has been shown to work well with uni-spectral extraction [25]. Our work
304 shows that the beam profile after the guide in general is similar to that of
305 uni-spectral extraction. It should therefore not be a problem to implement
306 a kink e.g. at 30 m and a second ellipse to get out of line of sight for longer
307 instruments.

308 Another option that is considered for many instruments is to use a feeder
309 (converging guide and a pinhole) to compress the beam for a chopper at 6
310 m. Indeed, the recent work presented in Ref. [26] shows that bi-spectral
311 extraction works well with a feeder, with performance nearly reaching that
312 of an elliptic guide. In short, every guide optical trick used by uni-spectral
313 extraction should still work for bi-spectral extraction.

314 To carry out these simulations, an improved model for reflectivities has
315 been implemented in McStas and VITeSS, and two new McStas components
316 have been written and tested: a mirror that correctly takes absorption into
317 account and an elliptic guide wall. We have also, based on Ref. [22], further
318 developed a method to ensure correct propagation of the neutrons when the
319 order of components is not uniquely defined, as is the case here. Finally,
320 we have implemented a general method to include two (or more) different
321 moderators in McStas. The McStas instrument file, these components and
322 files containing the parameters found in the optimizations presented will

323 be made available on the McStas website [11] and can also be obtained by
324 contacting the main author.

325 It is interesting to note that most of the mirror is placed outside the
326 guide: even when the starting parameters for the optimizations were with
327 the mirror firmly inside the guide, as in Fig. 1 b, the optimizer would converge
328 to having the mirror outside the guide, as in Fig. 1 c. Also, our simulations
329 show that the optimal guide set-up is not with a square cross section, but
330 rather a rectangle that is taller than it is wide. If a square cross-section is
331 forced, this decreases the performance significantly.

332 We can finally conclude that obtaining a wide wavelength band using bi-
333 spectral extraction is indeed feasible using elliptic guides for both long and
334 short instruments. The beam profile is homogeneous at the sample, and the
335 divergence is smooth and symmetric.

336 **Acknowledgement**

337 We thank Ken H. Andersen, Pascale Deen, and Kaspar H. Klenø for
338 engaging in discussion on the article subject and commenting on results.
339 We thank Peter K. Willendrup and Emmanuel Farhi for technical help with
340 software and the ESS-DMSC for providing computing power. We thank
341 Swiss Neutronics for providing data for the model of the mirror. We thank
342 the Danish Agency for Research and Innovation and Bundesministerium für
343 Bildung und Forschung (BMBF) for their support through the contribution
344 to the ESS update phase.

345 **References**

346 **References**

- 347 [1] ESS website. <http://ess-scandinavia.eu/>.
- 348 [2] Kaspar Hewitt Klenø, Klaus Lieutenant, Ken H. Andersen, and Kim
349 Lefmann. Systematic performance study of common neutron guide ge-
350 ometries. *Nuclear Instruments and Methods in Physics Research Section*
351 *A: Accelerators, Spectrometers, Detectors and Associated Equipment*,
352 696(0):75–84, 2012.
- 353 [3] Phillip M. Bentley, Shane J. Kennedy, Ken H. Andersen, and F. R.
354 David. Correction of Optical Aberrations in Elliptic Neutron Guides.
355 2001.
- 356 [4] L.D. Cussen, D. Nekrassov, C. Zendler, and K. Lieutenant. Multiple
357 reflections in elliptic neutron guide tubes. *Nuclear Instruments and*
358 *Methods in Physics Research Section A: Accelerators, Spectrometers,*
359 *Detectors and Associated Equipment*, pages 1–11, December 2012.
- 360 [5] F. Mezei and M. Russina. Neutron-optical component array for the
361 specific spectral shaping of neutron beams or pulses. *Patent US*, 7030397
362 B2 (2006).
- 363 [6] F. Mezei and M. Russina. Neutronenoptische Bauelementenanordnung
364 zur gezielten 242 spektralen Gestaltung von Neutronenstrahlen oder
365 Pulsen. *Patent Germany Amtl. Aktz.*, 102 03 591 (2002), 2002.

- 366 [7] F. Mezei. Advances by innovation and building on experience. *The ESS*
367 *project Vol II, New Science and Technology for the 21st Century (2002)*,
368 2002.
- 369 [8] K. Lieutenant J. Peters and F Mezei. Monte Carlo simulation of the
370 new time-of-flight powder diffractometer EXED at the Hahn-Meitner-
371 Institut. *Journal of Neutron Research*, 14(2):147–165, 2006.
- 372 [9] L. D. Landau and E. M. Lifshitz. *Statistical Physics*, volume 5 of *Course*
373 *of Theoretical Physics*. Butterworth-Heinemann, third edition, 1980.
- 374 [10] Kim Lefmann and K. Nielsen. McStas, a general software package for
375 neutron ray-tracing simulations. *Neutron News*, 10/3:20–23, 1999.
- 376 [11] McStas website. <http://www.mcstas.org/>.
- 377 [12] Klaus Lieutenant, Geza Zsigmond, Sergey Manoshin, Michael Fromme,
378 Heloisa N Bordallo, Dickon Champion, Judith Peters, and Ferenc Mezei.
379 Neutron instrument simulation and optimization using the software
380 package VITESS. pages 134–145, 2004.
- 381 [13] VITESS website. <http://www.helmholtz-berlin.de/vitess>.
- 382 [14] E. Farhi. The iFit data analysis library.
- 383 [15] E. Farhi, Y. Debab, and P. Willendrup. iFit. *J. Neut. Res.*, (17), 2012.
- 384 [16] DMSC website. <http://www.ess-dmsc.eu>.
- 385 [17] HZB cluster dirac. <http://www.helmholtz-berlin.de/angebote/it/dienste/dirac/index>
- 386 [18] Swiss Neutronics website . <http://www.swissneutronics.ch/products/coatings.html>.

- 387 [19] Andreas Houben, Werner Schweika, Thomas Brückel, and Richard Dron-
388 skowski. New neutron-guide concepts and simulation results for the
389 POWTEX instrument. *Nuclear Instruments and Methods in Physics
390 Research Section A: Accelerators, Spectrometers, Detectors and Associ-
391 ated Equipment*, 680:124–133, July 2012.
- 392 [20] K. H. Klenø and K Lefmann. Optimization of supermirror guide coating.
393 *In preparation*.
- 394 [21] Andreas K. Freund. Cross-sections of materials used as neutron
395 monochromators and filters. *Nuclear Instruments and Methods in
396 Physics Research*, 213(2–3):495–501, 1983.
- 397 [22] Peter K Willendrup, Linda Udby, Erik Knudsen, Emmanuel Farhi, and
398 Kim Lefmann. Using McStas for modelling complex optics, using simple
399 building bricks. *Nuclear Instruments and Methods in Physics Research
400 Section A: Accelerators, Spectrometers, Detectors and Associated Equip-
401 ment*, 634(1, Supplement):S150 – S155, 2011.
- 402 [23] Steve Peggs, editor. *Conceptual Design Report*. 2012.
- 403 [24] Kaspar Hewitt Klenø. Effects of Misalignment on Long Elliptical Guides.
404 *Report (unpublished)*, 2012.
- 405 [25] L.D. Cussen, D. Nekrassov, C. Zendler, Th. Krist, and K. Lieutenant.
406 An Improved Elliptic Neutron Guide Design for ESS. *In preparation*.
- 407 [26] C. Zendler, K. Lieutenant, D. Nekrassov, L.D. Cussen, and M. Strobl.
408 Bi-spectral beam extraction in combination with a focusing feeder. *Nu-*

409 *clear Instruments and Methods in Physics Research Section A: Acceler-*
410 *ators, Spectrometers, Detectors and Associated Equipment*, pages 1–8,
411 December 2012.